Purinergic Signalling (2016) 12:161–174
DOI 10.1007/s11302-015-9490-3

ORIGINAL ARTICLE

Saffron reduces ATP-induced retinal cytotoxicity by targeting P2X7 receptors

Lucia Corso[1,2] · Anna Cavallero[1] · Debora Baroni[1] · Patrizia Garbati[1] · Gianfranco Prestipino[1] · Silvia Bisti[2] · Mario Nobile[1] · Cristiana Picco[1]

Received: 22 July 2015 / Accepted: 15 December 2015 / Published online: 7 January 2016

Abstract P2X7-type purinergic receptors are distributed throughout the nervous system where they contribute to physiological and pathological functions. In the retina, this receptor is found in both inner and outer cells including microglia modulating signaling and health of retinal cells. It is involved in retinal neurodegenerative disorders such as retinitis pigmentosa and age-related macular degeneration (AMD). Experimental studies demonstrated that saffron protects photoreceptors from light-induced damage preserving both retinal morphology and visual function and improves retinal flicker sensitivity in AMD patients. To evaluate a possible interaction between saffron and P2X7 receptors (P2X7Rs), different cellular models and experimental approaches were used. We found that saffron positively influences the viability of mouse primary retinal cells and photoreceptor-derived 661W cells exposed to ATP, and reduced the ATP-induced intracellular calcium increase in 661W cells. Similar results were obtained on HEK cells transfected with recombinant rat P2X7R but not on cells transfected with rat P2X2R. Finally, patch-clamp experiments showed that saffron inhibited cationic currents in HEK-P2X7R cells. These results point out a novel mechanism through which saffron may exert its protective role in neurodegeneration and support the idea that P2X7-mediated calcium signaling may be a crucial therapeutic target in the treatment of neurodegenerative diseases.

✉ Cristiana Picco
picco@ge.ibf.cnr.it

[1] National Research Council, Institute of Biophysics, Via De Marini 6, 16149 Genoa, Italy

[2] Department of Biotechnology and Applied clinical Science, DISCAB, University of L'Aquila, L'Aquila, Italy

Keywords P2X7 receptor · Retinal cells · Saffron · Neurodegenerative disease

Abbreviations

AMD	Age-related macular degeneration
BzATP	3′-*O*-(4-benzoylbenzoyl) ATP
BBG	Brilliant Blue G
MTT	3-(4,5-Dimethylthiazol-2-yl)-2,5diphenyltetrazolium bromide
P2X7R	P2X7 receptor

Introduction

The importance of ATP in biological systems is universally known. In addition to being a source of energy for the cell, extracellular ATP can act as a neurotransmitter in the nervous system. Recently, it has been observed that the purinergic system can induce cell death within the central nervous system (CNS). In the retina, purines are involved not only in signaling between the different cell types [1], but high levels of extracellular ATP also produce retinal neurodegeneration [2–4]. Different studies demonstrated that both P2X and P2Y purinoceptors are expressed in various retinal cell types, such as photoreceptors, retinal ganglion cells, bipolar cells, and Muller cells [5–7]. P2Y are transmembrane G protein-coupled receptors while the P2X receptors form ATP-gated ion channels and are distributed in many cell types and tissues. To date, seven different P2X subunits (P2X1-7), which assemble into homotrimeric and/or heterotrimeric proteins, have been found [8]. Among these subtypes, P2X7 receptor (P2X7R) plays an important role. This receptor is present in immune cells and in the CNS, including the retina [9–12], and it has been proposed as a potential therapeutic target in CNS

disorders, such as Alzheimer's disease, neuropathic pain, and spinal cord injury by regulating the levels of intracellular calcium ($[Ca^{2+}]_i$) and interleukin-1β, and by activating multiple caspases (see for review [13]). This receptor is characterized by two states of permeability [14], both inducing a $[Ca^{2+}]_i$ elevation that could be critical for the biology of the cell. Zhang and colleagues [15] demonstrated in in vitro experiments that stimulation of P2X7R by the potent agonist 3′-*O*-(4-benzoylbenzoyl) ATP (BzATP) produced robust elevations in the Ca^{2+} level inside rat retinal ganglion cells, leading the cells to apoptosis. Furthermore, they showed that this damage was inhibited by the selective P2X7R antagonist Brilliant Blue G (BBG). Similarly, Notomi and co-authors [16] suggested that photoreceptor cell apoptosis induced by ATP was prevented by BBG.

Saffron (*Crocus sativus* L.) is a species belonging to the Iridaceae family and has been widely used as an herbal medicine and spice since ancient times [17]. Chemically, saffron stigmas contain more than 150 volatile and many non-volatile active components, including vitamins, sugars, minerals, various α- and ß-carotenes, carotenoids (zeaxanthin and crocetin), and crocins derived by crocetin esterification with sugars. Its flavor arises from safranal, which is present in the glycoside picrocrocin. However, saffron cultivars coming from different areas all over the world may differ in their characteristics which may lead to pronounced differences in the general composition of extracts. This could explain the variety of effects and discrepancies found in the literature. Pharmacological studies have demonstrated that saffron (Saf) and its constituents protect against damage, exerting anti-ischemic [18], anxiolytic [19], anti-inflammatory [20], and antitumor [21] properties. Maccarone et al. [22] provided data showing that Saf is protective in a rat model of light-induced retinal degeneration. A proof-of-principle clinical trial in age-related macular degeneration (AMD) patients confirmed the potentiality of Saf treatment in neurodegenerative diseases and its consistency in time [23, 24] and in patients carrying genetic mutations [25]. The biological mechanisms underlying neuroprotection are thus far unknown even though a direct control of gene expression was suggested [26, 27]. Despite the large number of causes of photoreceptor degeneration, the final pathways leading to photoreceptor death are similar. Elevations in $[Ca^{2+}]_i$ originate the activation of degradative proteases, such as calpains, which can induce photoreceptor apoptosis. In photoreceptors of a mouse model of retinal degeneration (rd1), intracellular Ca^{2+} levels increased to approximately 190 % compared with control photoreceptors [28].

The aim of this work was to investigate whether one of the possible ways of Saf neuroprotective action may be related to the modulation of purinergic receptors. To avoid using saffrons coming from different cultivars that may present different composition of the extract, in this paper, we used only saffron derived from Hortus Novus (L'Aquila, Italy), whose chemical characteristics has been analytically examined in previous studies. We tested Saf on two different cell models, primary mouse retinal cells and retina-derived mouse 661W cell line, stressed by relatively high ATP concentrations. The last cell line derived from retinal tumors of a transgenic mouse line and showed biochemical and cellular properties of retinal photoreceptors. Moreover, these cells have been shown to respond to a variety of toxic stimulation and to oxidative and light stresses by activating the same apoptotic program of normal retinal photoreceptor cells [29]. We evaluated the possible interaction between Saf and purinergic P2X receptors, particularly P2X7R. Different experimental approaches were used to analyze the Saf effect on retina-derived mouse 661W cell line and HEK293 cell lines stably expressing rat P2X7 (HEK-P2X7R) and P2X2 (HEK-P2X2R) receptors. Interestingly, Saf increased the cell viability after ATP treatment and inhibited the ATP-mediated $[Ca^{2+}]_i$ elevation on 661W cells and on HEK-P2X7R but not on HEK-P2X2R cells. Patch-clamp experiments confirmed the block induced by Saf on HEK-P2X7R cationic currents.

Materials and methods

Cell cultures

Primary retinal cell cultures were prepared using 2-week-old C57BL/6 mice. The experiments were performed in compliance with the Animal Care and Use Committee guidelines and in accordance with the ARVO Statement for the Use of Animals in Ophthalmic and Vision Research. The retina was detached, suspended in cold Hanks balanced salt solution (HBSS; Gibco—Life Technologies, Italy), and incubated at 37 °C in activated papain solution (0.06 mg/ml [Sigma-Aldrich, Milan, Italy] prepared in Neurobasal-A medium (NB; Gibco). After 20 min, 2 ml of 2 % fetal bovine serum (FBS) in NB was added for 5 min to stop the enzymatic reaction and tissue aggregates were eliminated by the addition of 200 μl DNase I (Sigma-Aldrich). FBS was aspirated and NB supplemented with 2 % B27 (Gibco) and 0.5 mM L-glutamine (Gibco) was added to tissue. To dissociate the cells, the papain-treated retina was gently manually pipetted (50 times) using a Pasteur pipette. Tissues were allowed to settle for 2 min and supernatant containing the dissociated cells was collected. After the dissociation, the cells were seeded at 1×10^4 cells in 96-well plates and incubated for 4–5 days before experiments.

The mouse retinal photoreceptor-derived 661W cell line (kindly provided by Dr. Muayyad Al-Ubaidi (University of Oklahoma Health Sciences Center, OK, USA)) was cultured in Dulbecco minimum essential medium supplemented with

10 % FBS, 10 % L-glutamine, 100 units/ml penicillin, and 100 μg/ml streptomycin (Gibco).

Human embryonic kidney cell line HEK293 was stably transfected with a pcDNA3 plasmid containing the full length rat P2X7-GFP cDNA, as described previously [30]. HEK293 cells stably transfected with rat P2X2 were kindly provided by Prof. Surprenant (University of Manchester, UK). Cells were maintained in Dulbecco's modified Eagle's medium/Nutrient Mixture F-12 Ham supplemented with 10 % FBS, 5 mg/ml gentamycin and 200 mM glutamine. Confluent cells were replated on 20-mm glass coverslips at a density of 5×10^3 for Ca^{2+} and current measurements and in 96-well plates for viability tests.

Viability assay

Confluent cultures were subcultured in 96-well culture plates at a density of 5×10^3 cells/well and allowed to attach for 24 h. Saffron (L'Aquila Saffron, Italy) used in the present paper has the same chemical characteristics (defined by HPLC analysis) as the saffron tested in animal models and human AMD patients [27] and has been patented (Hortus Novus S.r.l.). Stigmas of saffron were crushed and dissolved in water at a concentration of 5 mg/ml 18–24 h before cell treatment. Cells were incubated with different Saf and ATP or BzATP concentrations. Cell viability was assessed by measuring the reduction of 3-(4,5-dimethylthiazol-2-yl)-2,5diphenyltetrazolium bromide (MTT) (Sigma-Aldrich) after 24 h of ATP treatment. MTT solution (5 mg/ml in phosphate-buffered saline (PBS)) was added for 2 h resulting in formazan formation, which was solubilized with DMSO (100 μl). The absorption at 570 nm was measured using a FLUOstar Omega micro-plate reader.

Determination of apoptosis by fluorescence microscopy

Apoptosis/necrosis tests were done on 661W cells using the GFP-Certified Apoptosis/Necrosis detection kit (Enzo LifeSciences). Cells were seeded on glass slides at 80 % confluency and treated for 24 h with ATP (5 or 10 mM) with and without the addition of 25 μg/ml Saf. Slides were washed with PBS and incubated for 15 min in the dual detection reagent containing apoptosis (Annexin V) and necrosis (7-AAD) detection reagent in 1× binding buffer. The samples were incubated at room temperature in the dark. After staining, the cells were washed with binding buffer and observed under a Leica SP2 confocal microscope with dual filter set for Annexin V (Ex/Em 550/570) and for 7-ADD (Ex/Em 546/647).

Western blot

The mouse retinal photoreceptor-derived 661W cell, the control HEK293 cells, and HEK293 cells stably transfected with P2X7R-EGFP were lysed in a buffer containing 62.5 mM Tris, 2 % sodium dodecyl sulfate (SDS), and a cocktail of protease inhibitors (1 mM 4-(2-aminoethyl)benzenesulfonyl fluoride hydrochloride (AEBSF), 0.8 μM aprotinin, 0.2 μM leupeptin, 40 μM bestatin, 15 μM pepstatin A, 14 μM E-64). Samples were sonicated for 2 s and heated at 98 °C for 5 min. Protein concentration was determined using the method of Lowry [31] with bovine serum albumin as the standard. Equal amounts of proteins (15 μg) were subjected to SDS polyacrylamide gel electrophoresis analysis. Separated proteins were transferred to PVDF membrane (Millipore, Billerica, Massachusetts, USA) for 1 h. The blots were then incubated with a polyclonal antibody against an intracellular epitope of P2X7R (1:500; Alomone Labs, Jerusalem, Israel) as primary antibody and with horseradish peroxidase-conjugated goat anti-rabbit antibody (1:4000, Santa Cruz, Santa Cruz, CA, USA) as secondary antibody. Immunodetection was performed using Amersham ECL PLUS detection reagents and the images were captured by using Amersham Hyperfilm ECL. Developed films (Kodak, Rochester, NY, USA) were scanned using a flat-bed scanner with a resolution of 600 dpi. In order to confirm the homogeneity of the loaded proteins, immunoblots were stripped by incubating them with stripping buffer (62.5 mM Tris pH 6.8, 10 % SDS, and 1 % β-mercaptoethanol for 30 min at 55 °C) and reprobed with a polyclonal anti-actin primary antibody (1:3000, Sigma-Aldrich).

Biotinylated 661W cell surface samples were incubated with the anti-intracellular epitope of P2X7 antibody (1:500; Alomone Labs, Jerusalem, Israel) as primary antibody and with horseradish peroxidase-conjugated goat anti-rabbit antibody (1:4000, Santa Cruz, Santa Cruz, CA, USA) as secondary antibody. Anti-pan cadherin antibody, which recognizes the plasma-membrane marker cadherin, was used as a gel loading control. In order to confirm the specificity of the anti-P2X7 primary antibody, whole lysate and membrane surface samples of 661W cells were pre-incubated in excess control antigen and analyzed by Western blot. Each experiment was conducted in triplicate.

Single-cell $[Ca^{2+}]_i$ microfluorimetry

Intracellular calcium measurements were performed by using the fluorescent Ca^{2+} indicator fura-2 AM. Cells were loaded with 5 μM fura-2 AM dissolved in extracellular solution for 45 min at 37 °C. Pluronic acid (0.1 %) was added to improve dye uptake. Cell coverslip was placed on the stage of an inverted fluorescence microscope Nikon TE200 (Nikon, Tokyo, Japan) equipped with a dual excitation fluorometric calcium imaging system (Hamamatsu, Sunayama-Cho, Japan). The external standard solution was composed of (mM) 135 NaCl, 5.4 KCl, 1 $CaCl_2$, 5 Hepes, and 10 glucose at pH 7.3. Ca^{2+}-free standard solution was similar but Ca^{2+} was replaced

with 5 mM EGTA. Crocins from Sigma (Sigma-Aldrich) were dissolved in water at a concentration of 10 mg/ml. To obtain crocetin, 1 ml HCl (12 M) was added to a solution containing crocins or saffron for 30 min at 37 °C; pH was increased to 7 with NaOH.

Fluorescence emission was acquired with a digital CCD camera (Hamamatsu C4742-95-12ER). Monochromator settings, chopper frequency, and data acquisition were controlled by dedicated software (Aquacosmos/Ratio U7501-01, Hamamatsu). The sampling rate was 0.25 or 0.5 Hz. Fura-2 AM-loaded cells were excited at 340 and 380 nm and fluorescence emission measured at 510 nm. The fluorescence ratio F340/F380 was used to monitor $[Ca^{2+}]_i$ changes. In some experiments, $[Ca^{2+}]_i$ was calculated according to Grynkiewicz [32], using a K_D of 140 nmol/l for the Ca^{2+}/fura-2 complex.

Current measurements

The electrophysiological studies were performed at room temperature (20–22 °C) using the whole-cell configuration of the patch-clamp technique. Patch pipettes were pulled from borosilicate glass capillaries (Clark Electromedical Instruments) and heat-polished to obtain a resistance of 2–4 MΩ when filled with pipette solution. The external standard solutions were the same as those used for intracellular calcium measurements. The standard pipette solution contained (mM) 135 NMDG-Cl, 1 $MgCl_2$, 5 Hepes, 5 EGTA, and 5 glucose at pH 7.3. Membrane currents were recorded using an AXOPATCH 200A patch-clamp amplifier (Axon Instruments) and were filtered at 1 kHz before acquisition. Both voltage stimulation and data acquisition were obtained using a 12-bit interface (Axon Instruments) and a microcomputer equipped with pClamp 10.2 software. Experiments were performed at a holding potential of −60 mV with stimulation protocol of 90-ms length.

Statistics

All data are given as means ± SEM from at least four experiments. The statistical significance of differences between mean values was assessed using Student's *t* test. Differences were regarded as statistically significant for $*p<0.05$ and $**p<0.01$.

Results

Saffron decreases retinal photoreceptor apoptosis induced by extracellular ATP

We evaluated in in vitro experiments the efficiency of saffron extract (Saf) in mitigating ATP stress by using two different mouse retinal cell cultures, primary retinal cells, and mouse retinal photoreceptor-derived 661W cells. In previous reports, 661W cells have been used as a cellular model to investigate the mechanisms involved in photoreceptor degeneration [33]. Both cell cultures were stressed by using ATP concentrations ranging from 1 to 10 mM. The neuroprotective effects of Saf were tested using a MTT assay (see Fig. 1). Cells were incubated with Saf 25 μg/ml and ATP at concentrations of 1, 5, and 10 mM for 24 h. As observed from experiments, Saf alone did not produce any significant difference in cell viability (97 %) with respect to control (Fig. 1a); moreover, increasing Saf concentrations from 5 to 500 μg/ml in the presence of extracellular ATP did not increase cell viability (Fig. 1c), whereas the effect of ATP was concentration dependent in both cell types (Fig. 1a, b). On primary retinal cultures, 1 mM ATP had no effect on cell viability, while at 5 mM the percentage of live cells was reduced to about 57 % compared to untreated control cells (Fig. 1a). Saffron was significantly protective against 5 mM ATP stress, shifting the cell viability to about 77 %, respectively ($p<0.01$). A smaller but still significant effect of Saf was seen when the primary culture of retinal cells was incubated with a higher concentration of ATP (10 mM): treatment with Saf increased cell viability from about 34 to 43 % ($p<0.01$).

The mouse retinal photoreceptor-derived 661W cells presented a higher sensitivity to stress induced by external ATP; cell viability decreased to 79 % at 1 mM, to 44 % at 5 mM, and to 8 % at 10 mM ATP (Fig 1b). In the presence of 1 mM ATP, the analysis showed a mild, but statistically significant, effect of Saf ($p<0.01$). Viability values of 661W cell with Saf treatment (Saf *plus* ATP 5 mM) significantly increased to 54 % ($p<0.05$). When the cells were incubated with a higher concentration of ATP (10 mM), Saf showed also a significant protection ($p<0.01$). The number of living cells after treatment of 5 mM ATP and Saf plus ATP was evaluated also by using fluorescence microscopy. Cells were stained with DAPI to visualize the nuclei of living cells (Fig. 1d). In the presence of ATP alone (Fig. 1d—middle panel), cells were less numerous than those treated with Saf plus ATP (right panel). The number of fluorescent nuclei was evaluated in each condition and normalized to the number of stained nuclei of control cells, and results were plotted in Fig. 1d (last panel).

It is known that ATP induces apoptosis in retinal cells [34]; therefore, Annexin V assays (see "Materials and methods" section) were used on 661W cells in order to distinguish whether ATP treatment produced necrosis or apoptosis in this cellular model. In addition, we evaluated the efficiency of the incubation with Saf on mitigating cell apoptosis induced by ATP. Figure 2 shows the images of 661W cells in control condition (a), stressed by 10 mM ATP (b), and in the presence

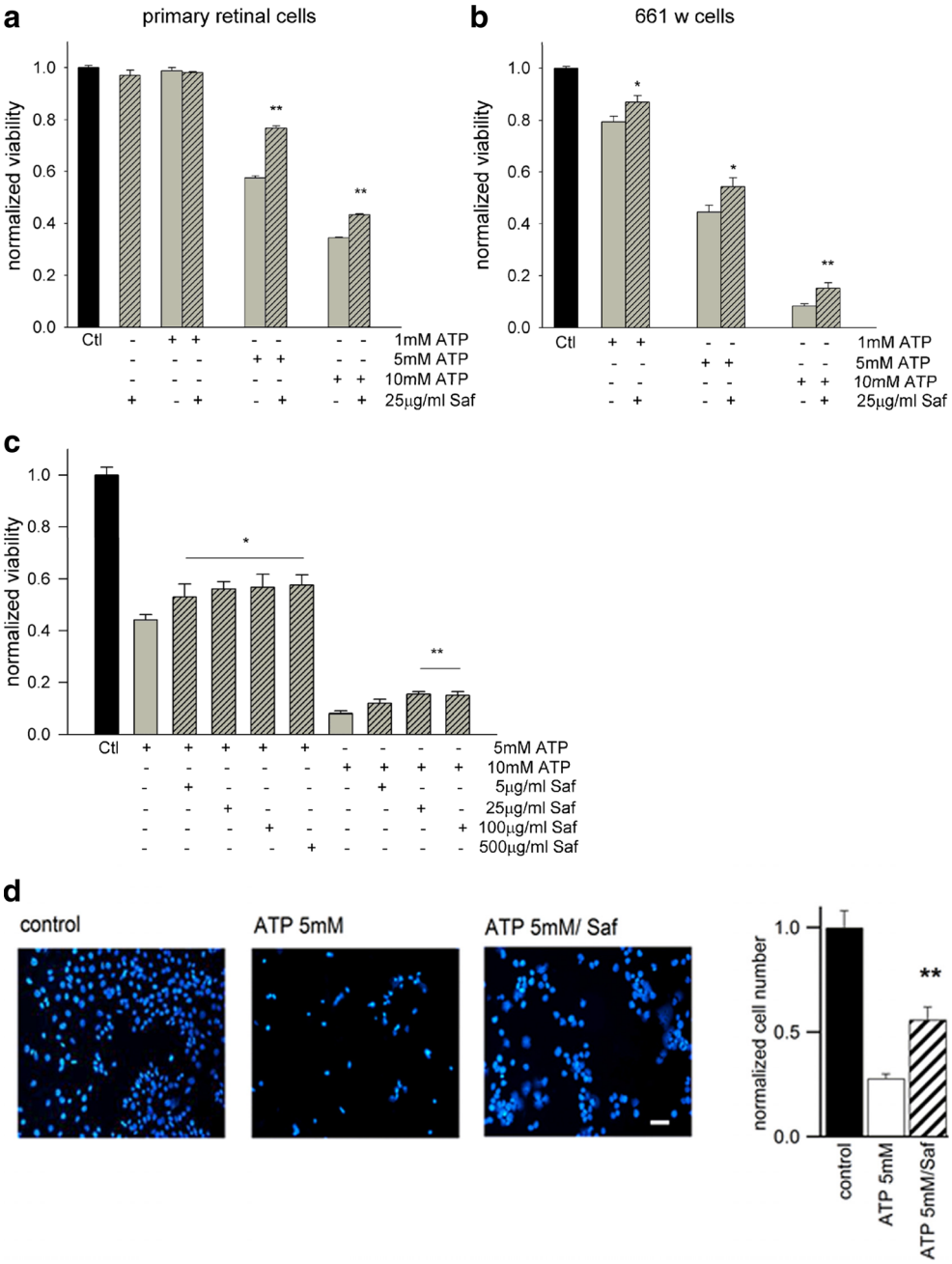

Fig. 1 Saf increases the viability of retinal cells treated with extracellular ATP. Cytotoxic effect in **a** primary mouse retinal cultures and in **b** mouse retinal photoreceptor-derived 661W cells induced by application of 1, 5, and 10 mM ATP for 24 h and in co-treatment of ATP *plus* Saf (25 μg/ml). **c** Dependence of cell viability (after treatment with 5 and 10 mM ATP) on Saf concentrations. Viable cells were counted using MTT assay and normalized to control cells. Differences between treatment of ATP and ATP *plus* Saf were significant being taken at $*p < 0.05$ and $**p < 0.01$. **d** DAPI imaging of nuclei of untreated cells (*left panel*), after treatment with ATP (*central panel*) and after co-treatment with ATP and 25 μg/ml Saf (*right panel*). *Scale bar* = 25-μm. Data are obtained in triplicate from at least four different experiments

of Saf (25 μg/ml) plus ATP (10 mM) (c). As observed with confocal fluorescence microscopy, treatment with extracellular ATP induced apoptosis (in early and late stage) in 661W cells (Fig. 2b–d). On the contrary, no significant necrosis was observed at both ATP concentrations (less than 2 % in cells treated with 5 and 10 mM ATP). Moreover, the incubation with Saf decreased significantly the number of apoptotic cells (Fig. 2c), but had no effect on the number of necrotic cells. Figure 2e summarizes the results obtained in the different conditions (5 and 10 mM ATP with and without Saf incubation). As expected, increasing the amount of ATP augmented the number of apoptotic cells.

Saffron reduces P2X7R-mediated calcium entry in ATP-treated retinal photoreceptor-derived 661W cells

Several studies reported the critical involvement of ATP-activated P2X7 purinoceptors in retinal neurodegeneration [15, 16, 35]. As previously mentioned, P2X7Rs are expressed in the majority of retinal cell types, such as photoreceptors, ganglion cells, and bipolar cells. On the contrary, until now there is no evidence for the presence of this receptor on 661W cells. We verified the expression of P2X7Rs in 661W cell line by using Western blot analysis. In order to validate the functionality of the antibody, the HEK293 cell line either

untransfected or stably transfected with the rat P2X7R-GFP was used. Figure 3a reveals a band of 68 kDa in 661W cells and a band of 95 kDa in HEK293-P2X7R-GFP cells, which correspond to the expected molecular weight of the P2X7 receptor subunit alone and plus GFP, respectively. Vice versa, this band was completely absent in untransfected HEK293 cell line; actin was used as a control housekeeping protein for the different cell lines. Moreover, cell surface biotinylation assay on 661W cells allows us to recognize the presence of the full-glycosylated P2X7 protein on the plasma membrane of this cell line (Fig. 3b). In both kinds of experiments, the specificity of the antibody for its target was further demonstrated by the complete obliteration of staining when the antibody was pre-incubated in excess control antigen. After proving the presence of P2X7R on the plasma membrane of 661W cells, we investigated if saffron protected from stress induced by the potent P2X7 agonist BzATP (3′-*O*-(4-benzoyl)benzoyl-ATP). Cells were exposed to 400 μM BzATP for 24 h with saffron (25 μg/ml). The results in Fig. 3c show that 400 μM BzATP decreased 661W cell viability to about 60 % compared to the control. This result further confirms that P2X7 receptors are expressed in the 661W cell line. As observed for ATP, saffron significantly protected from BzATP damage, increasing cell viability to 76 % ($p < 0.01$).

Furthermore, we evaluated the P2X7R involvement on Saf protection from ATP stress by measuring the intracellular calcium $[Ca^{2+}]_i$ variations induced by external ATP in mouse retinal photoreceptor-derived 661W cells. Because 1 mM ATP produced a change of $[Ca^{2+}]_i$ only in 27 % of the cells (17/62), we increased the agonist concentration to 2 mM in these experiments. In fura-2-loaded 661W cells bathed with an extracellular control solution, a subsequent application of 2 mM ATP caused a relatively rapid increase in $[Ca^{2+}]_i$ that slowly attenuated to a lower level (Fig. 4a; $n = 87$ cells). On the contrary, when 2 mM ATP was applied in a nominally Ca^{2+}-free solution (no Ca^{2+}, 5 mM EGTA added), cells generally did not show a significant $[Ca^{2+}]_i$ elevation but a typical intracellular Ca^{2+} increase was observed switching to an extracellular solution containing 1 mM Ca^{2+} (Fig. 4b). Calcium imaging analysis showed that exposure of cultured 661W cells to 2 mM ATP in external 0 Ca^{2+} promoted a Ca^{2+} release from intracellular stores only in 18 % of the cells examined (10/54 cells). We then tested the effect of Saf on the ATP-induced $[Ca^{2+}]_i$. increase. The addition of Saf alone (25 μg/ml) did not induce any variations of the intracellular Ca^{2+} level (Fig. 4c), but a subsequent application (after 5 min) of 2 mM ATP elicited a lower $[Ca^{2+}]_i$ rise than that evoked

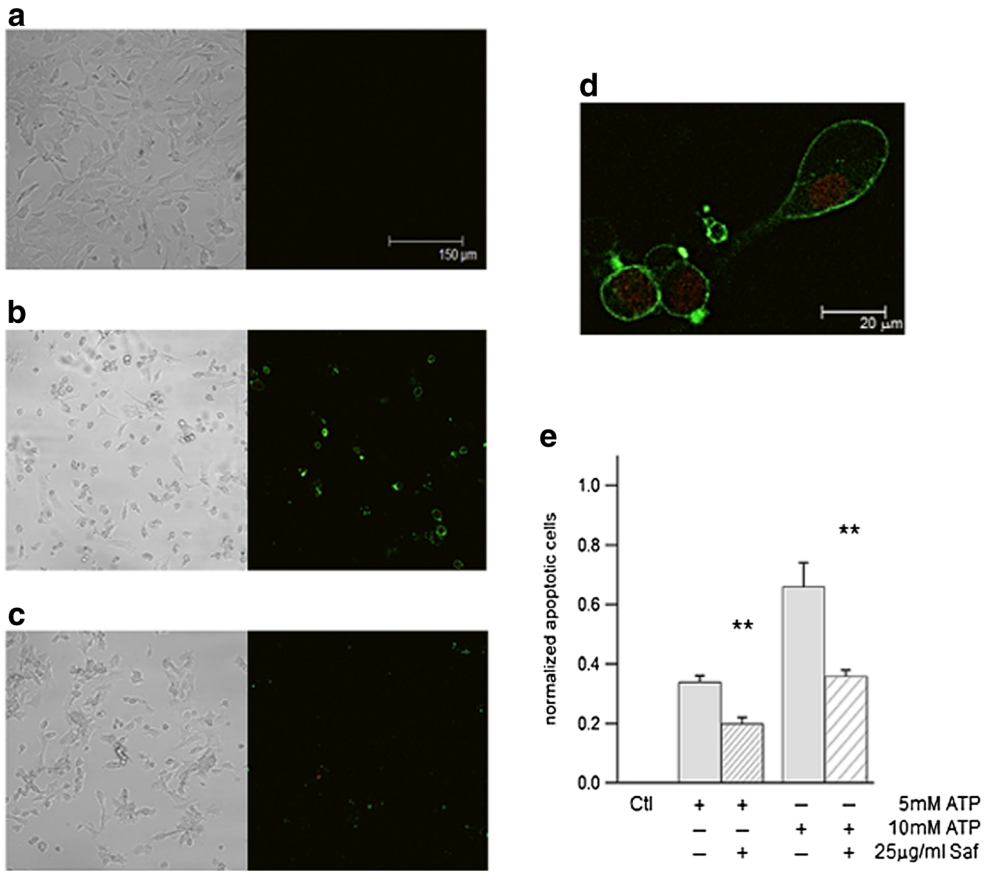

Fig. 2 ATP induces apoptosis in 661W cells. Confocal fluorescence images of 661W cells in **a** control condition, **b** after 24 h treatment of 10 mM ATP, and **c** co-treatment of ATP *plus* Saf (25 μg/ml). *Green cells* indicated early apoptosis while *green* and *red cells* showed late-stage apoptosis. Finally, *red cells* were necrotic. **d** Higher magnification of apoptotic and late apoptotic cells induced by the application of extracellular ATP; *scale bar* = 20-μm. **e** Bar graph resumes apoptosis effects in 661W cells at 5 and 10 mM ATP with or without the incubation of Saf. The number of apoptotic cells for each condition was normalized to the number of total cells present in each condition. Data are obtained in triplicate from at least four different experiments

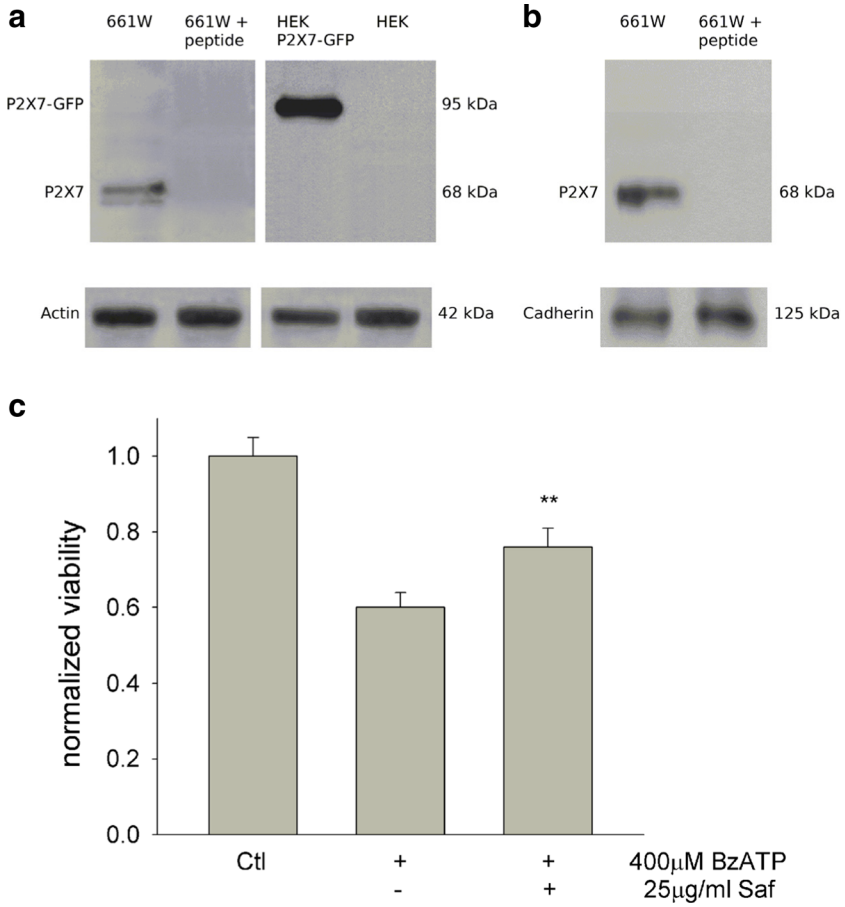

Fig. 3 Detection of P2X7R in 661W cell line. **a** The antibody anti-P2X7R detects P2X7 receptor in mouse retinal photoreceptor-derived 661W cells (*first line*), but no staining is observed when the antiserum is pre-incubated in excess control peptide (*second line*). A prominent band of 95 kDa, corresponding to P2X7-EGFP, is detected also in whole-cell lysates from P2X7-EGFP transfected HEK cells (*third line*). No signal is detected in whole-cell extracts from untransfected HEK cells (*fourth line*). Actin bands of 42 kDa detected on the same blotting membranes. **b** P2X7R is detected as a band of 68 kDa in the cell surface biotinylated fraction of 661W cells (*first lane*), while no signal is observed in the same fraction when the antiserum is pre-incubated in excess control peptide (*second lane*). The anti-pan cadherin antibody has been used to detect the plasma membrane marker cadherin. **c** Saffron increased 661W cell viability after treatment with the agonist BzATP (*$p < 0.05$)

by individual application of ATP (Fig. 4d). The results summarized in Fig. 4f showed that the ATP-induced $[Ca^{2+}]_i$ maximal response was inhibited by 43 % in the presence of Saf. Similar experiments were performed in the presence of the specific P2X7R antagonists A438079 (0.5 and 1 μM), oxidized ATP (oATP; 100 μM; pre-incubation for 2 h), or Brilliant Blue G (BBG; 1 μM) [36–38]. A438079 and BBG were applied 5 min before the addition of 2 mM ATP. The analysis showed that the ATP-induced $[Ca^{2+}]_i$ increase was inhibited in the presence of all three P2X7R antagonists (Fig. 4g). In particular, the calcium signal fully inhibited in the presence of 1 μM A438079 (Fig. 4e; first part of the trace) and completely recovered after the removal of the antagonist (Fig. 4e; the last part of the trace). These data indicate that P2X7R is critically implicated in ATP-induced $[Ca^{2+}]_i$ variations in retinal photoreceptor-derived 661W cells.

Saf effect on stress induced by ATP in HEK293 stably transfected with rat P2X7R

To confirm the involvement of P2X7Rs in Saf protection against ATP stress, we extended our analysis on HEK293 cells stably expressing rat P2X7Rs (HEK293-P2X7R). In parallel experiments, these cells were exposed to either the natural agonist ATP or the synthetic one BzATP. It is known that both ATP and BzATP responses differ between rat and mouse P2X7R: rat P2X7R is 10 times more sensitive to ATP and 100 times more sensitive to BzATP than mouse P2X7R [39]. Based on these considerations and on previous results on rat HEK293-P2X7R [30], we used 250 μM ATP and 10 μM BzATP to reduce cell viability to approximately 60 %. In Fig. 5a, HEK293-P2X7R cells in control condition are shown and compared to cells treated for 24 h with ATP alone and with the addition of Saf.

The number of viable cells was estimated in the different conditions and normalized to that obtained in control condition. Similar to retinal cells, Saf protected from damage when it was incubated for 24 h with ATP; cell viability increased from 57 % with 250 μM ATP alone to 69 % with ATP plus Saf ($p < 0.01$; Fig. 5b). An analogous behavior was observed in the presence of BzATP. Figure 5c shows that the percentage of living cells exposed at 10 μM BzATP decreased to 66 % compared to control. Saf treatment for 24 h increased cell viability to 82 % ($p < 0.01$). Saf modulation was also compared to the activity of 1 μM of BBG, which selectively inhibits P2X7Rs [36]. The BBG inhibitor alone had only a minor effect reducing the cell viability to about 95 %, whereas when applied with BzATP, the viability value was about 88 % compared to the 82 % in the presence of BzATP plus Saf. This experiment demonstrated that the inhibitory effect of Saf on the P2X7R was similar to that of the specific antagonist BBG.

To better elucidate the specificity of Saf protection through its effects on P2X7R, we used HEK293 cells stably expressing the full-length rat P2X2 receptor, which in some properties is similar to P2X7R. Cells were exposed to 250 μM ATP, 30 μM BzATP, and ATP or BzATP plus Saf using the same experimental protocol used in the previous experiments. Both purines induced a decrease of cell viability compared to control similar to that observed for HEK293-P2X7R (Fig. 5d), but, differently from HEK293-P2X7R, Saf was not able to increase the cell viability of HEK-P2X2R. This experiment confirmed that Saf interacts with the P2X7R and not with P2X2R.

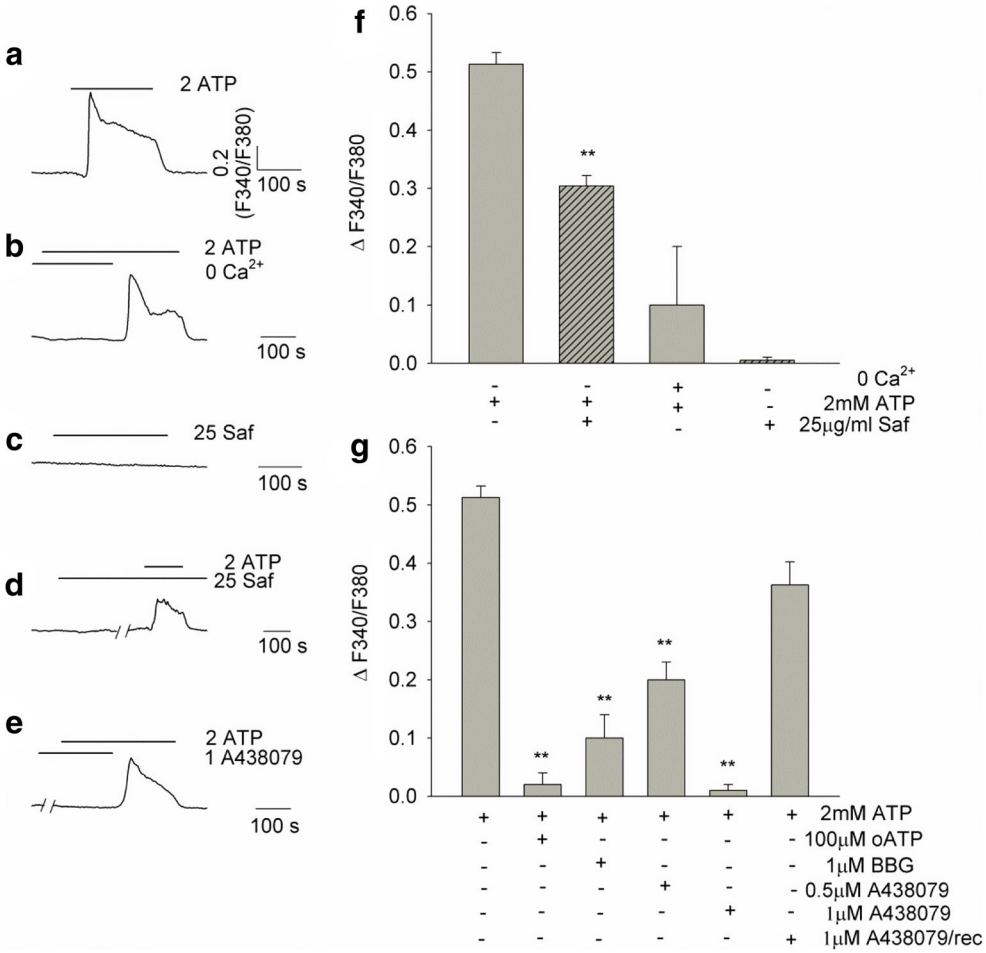

Fig. 4 Saf affects the ATP-induced $[Ca^{2+}]_i$ elevation in 661W cells. **a**–**e** Representative traces of single-cell fura-2 fluorescence ratio, indicative of $[Ca^{2+}]_i$ variation, in response to application of 2 mM ATP in control solution (**a**); 2 mM ATP in absence of extracellular Ca^{2+} and after switching to control solution (**b**); 25 μg/ml Saf alone (**c**); 2 mM ATP *plus* 25 μg/ml Saf (**d**); the $[Ca^{2+}]_i$ signal recovery after the reversible selective P2X7 antagonist A438079 (1 μM) removal (**e**). *Horizontal bars* indicate the time period of exposure. **f** Quantitative analysis of $[Ca^{2+}]_i$ maximal elevation above basal levels elicited by ATP in extracellular Ca^{2+}-free, control solution and in the presence of Saf. Differences between ATP and ATP *plus* Saf were significant $^{**}p < 0.01$. Data were obtained from at least 35 cells. **g** Inhibition of ATP-induced $[Ca^{2+}]_i$ elevation in the presence of the selective P2X7R antagonist A438079 (1 μM), oATP (100 μM) or BBG (1 μM). Differences between ATP and ATP *plus* Saf or blockers were significant ($^{**}p < 0.01$). Data were obtained from at least 33 cells

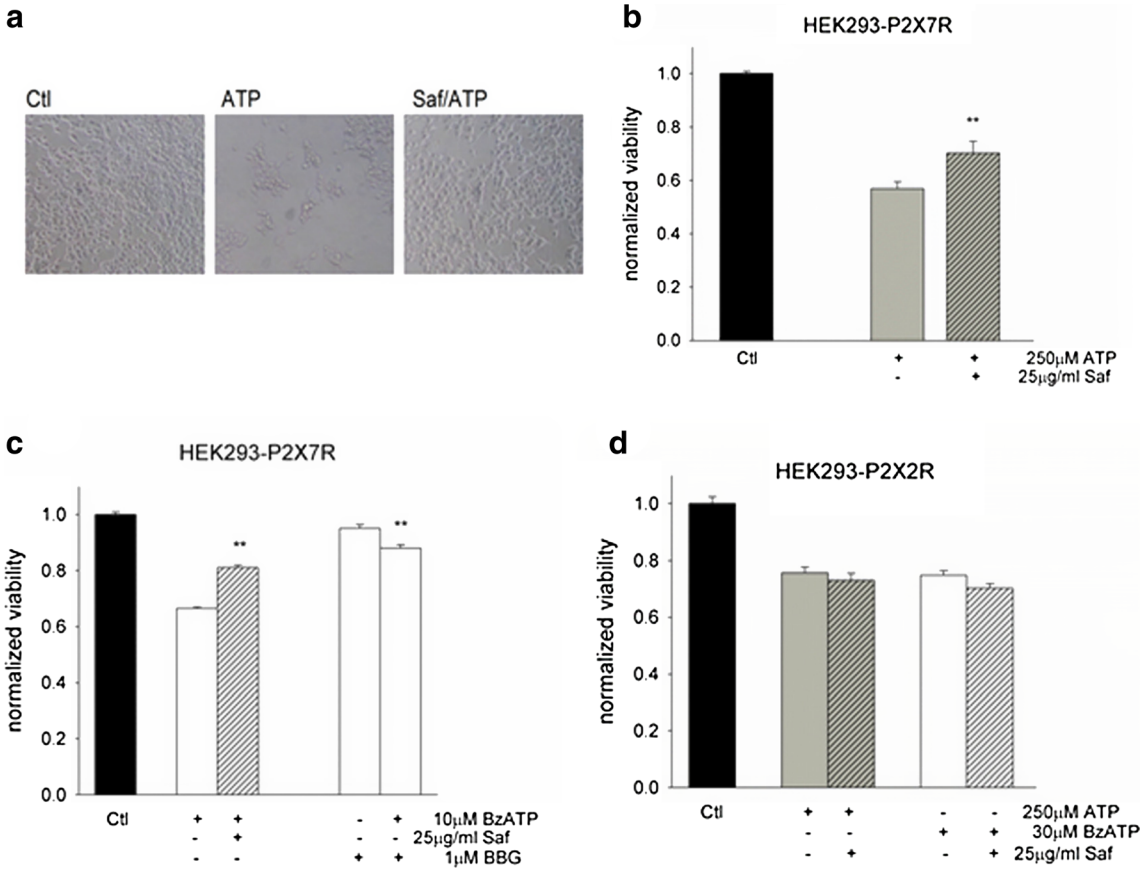

Fig. 5 Saf interaction with P2X7R expressed in HEK293 cells (HEK293-P2X7R). **a** Microphotographs of HEK293 cells stably transfected with P2X7R in control condition, after treatment with 250 μM ATP, after co-treatment with Saf (ATP *plus* Saf). **b** Viable cells were estimated from MTT test 24 h after the application of 250 μM ATP in different Saf conditions and normalized to control cells. **c** Cytotoxicity assay induced on HEK293-P2X7R cells by 10 μM BzATP for 24 h and with co-treatment with 25 μg/ml Saf. Differences between cells stressed by ATP or BzATP and ATP or BzATP with Saf were significant: $^{**}p < 0.01$. The bar graph also shows the significant blocking effect of 1 μM BBG in these experimental conditions. **d** Saf effect on HEK293 cells expressing the rat P2X2 receptor. Histogram illustrating the cell viability normalized to control cells after the application of 250 μM ATP or 30 μM BzATP and 25 μg/ml Saf. Data are obtained in triplicate from at least four different experiments

Saf inhibits the BzATP-evoked $[Ca^{2+}]_i$ rise in HEK293-P2X7R

In order to get insights into the mechanism of interaction between Saf and the ionotropic P2X7R, we analyzed the effect of Saf on BzATP-evoked intracellular calcium variations. It is known that HEK293 cells transfected with the full-length rat P2X7R challenged with micromolar concentrations of the relatively selective agonist BzATP exhibited a $[Ca^{2+}]_i$ signal elicited by Ca^{2+} influx through the P2X7R itself [30]. First of all, we verified the effect of Saf and BzATP, applied alone, on $[Ca^{2+}]_i$ variations. In fura-2-loaded HEK293-P2X7R, the application of 5 μg/ml Saf did not induce any Ca^{2+} increase (Fig. 6), whereas 3 μM BzATP promoted a biphasic $[Ca^{2+}]_i$ rise with a rapid and a slow $[Ca^{2+}]_i$ elevation. In the presence of Saf, a subsequent (after 5 min) BzATP application (3 μM) elicited a lower $[Ca^{2+}]_i$ rise than that evoked by individual application of BzATP, particularly affecting the slower component of the $[Ca^{2+}]_i$ elevation (Fig. 6 last trace). Similar experiments performed with the specific P2X7R antagonist BBG and by using different Saf concentrations were summarized in Fig. 6b. The results show that 100 nM BBG inhibited the BzATP-induced $[Ca^{2+}]_i$ increase by 90 %, whereas the maximal inhibitory effect of Saf was about 30 %. We tried different Saf concentrations: 1, 5, 10, 25 μg/ml. As shown in the histogram 5, 10, and 25 μg/ml gave the same effect on the BzATP-induced Ca^{2+} signal, so in all subsequent experiments, we used 5 μg/ml Saf. The effects of Saf were tested on different agonist concentrations. Figure 6c shows representative traces of $[Ca^{2+}]_i$ response induced by 20 μM BzATP alone and when the agonist was applied in the presence of 5 μg/ml Saf. The dose-response curves demonstrate that the maximal $[Ca^{2+}]_i$ elevation was obtained at 20 μM BzATP, whereas in the presence of Saf, the same concentration did not induce the maximum effect (Fig. 6d). The EC_{50} value was 1.1 μM and the Hill coefficient 2.1 in control conditions and 1.7 μM with a Hill coefficient of 1.5 in the presence of BzATP plus Saf. These results indicate that the values of the two EC_{50} were

not significantly different, but the maximal $[Ca^{2+}]_i$ elevation in the presence of Saf was strongly reduced, suggesting a non-competitive block of P2X7Rs.

Finally, we tested the effects of two potent antioxidant ingredients of saffron: crocins (CRN) and crocetin (CRT), a carotenoid dicarboxylic acid which forms the core of crocins. We found that both compounds interfered with calcium signaling of P2X7Rs. Figure 7 shows a representative trace of the $[Ca^{2+}]_i$ response induced by 3 μM BzATP alone (a) and in co-presence of 10 μg/ml CRN (b) and 10 μg/ml CRT (c). We tested the two carotenoids at two different concentrations, 10 and 25 μg/ml. As demonstrated by the histogram, both two carotenoids were more active at 25 μg/ml concentration and crocetin was found to be more active than crocin (Fig. 7d).

Saf modulated cationic currents on HEK293-P2X7R cells

Patch-clamp experiments were carried out on HEK293-P2X7R cells to verify the modulation induced by Saf on P2X7 channels. Cells were clamped at a holding potential of −60 mV and whole-cell inward currents were elicited in response to 3 μM BzATP (Fig. 8a). Upon repeated (every 3 min, 30 s long) applications of 3 μM BzATP, the evoked currents increased in magnitude and reached their maximal levels after four applications. After 5-min washout and in the presence of 5 μg/ml Saf (3 to 5 min), a subsequent application of 3 μM BzATP plus Saf induced a smaller inward current compared to the control condition (Fig. 8b). The current trace in panel c was representative of the recovery obtained after 5-min

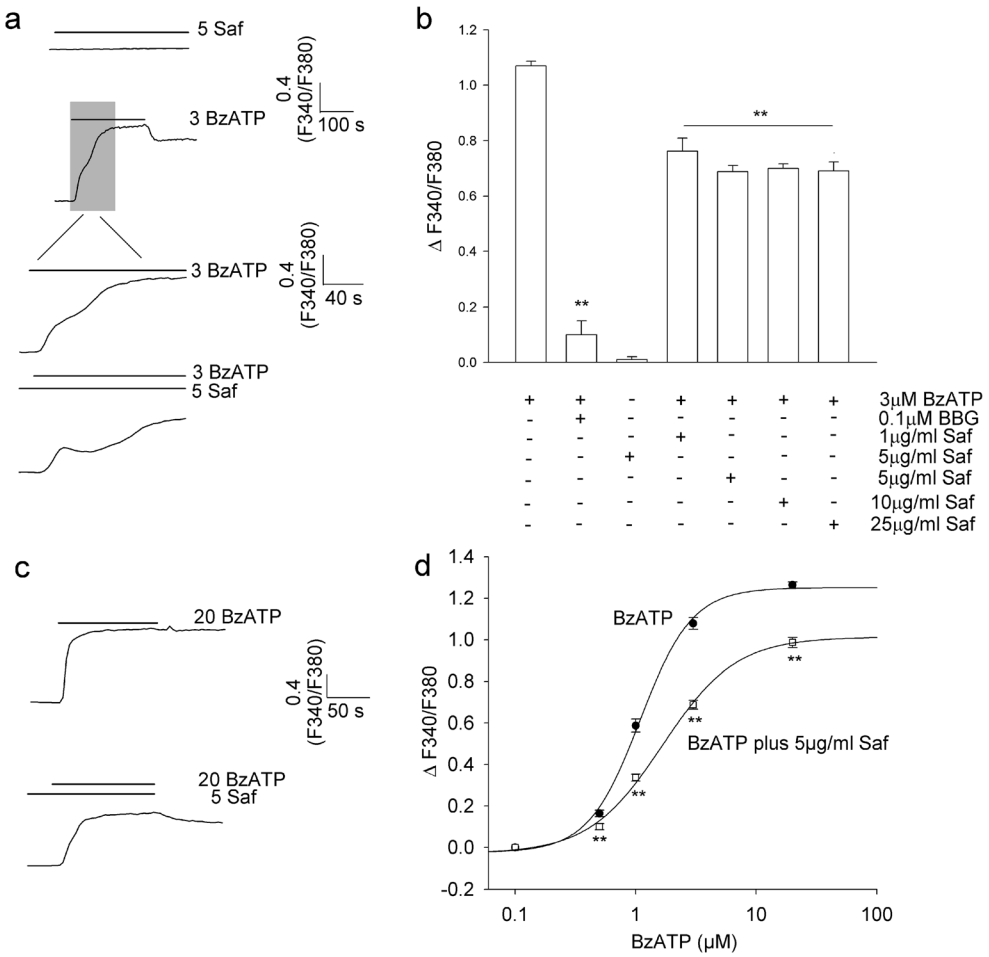

Fig. 6 Saf affects in a non-competitive manner the BzATP-induced $[Ca^{2+}]_i$ elevation in HEK293-P2X7R cells. **a** Representative traces of single-cell fluorescence ratio, indicative of $[Ca^{2+}]_i$ variation, in response to application of 5 μg/ml Saf alone (*first trace*) and 3 μM BzATP (*second trace*). BzATP promoted a biphasic $[Ca^{2+}]_i$ rise which is shown as a *gray area* and depicted on a larger scale (*third trace*). Same cell was exposed to 5 μg/ml Saf (5 min) and subsequently with 3 μM BzATP (*last trace*). *Horizontal bars* indicate the time period of Saf or BzATP applications. **b** The bar graph reports the concentration-dependent effect of Saf and the selective P2X7R antagonist BBG (100 nM) inhibition of $[Ca^{2+}]_i$ elevation induced by 3 μM BzATP. **c** Representative traces of single-cell fluorescence ratio depicting the $[Ca^{2+}]_i$ increase induced by 20 μM BzATP alone (*upper trace*) or BzATP *plus* 5 μg/ml Saf (*lower trace*). **d** Quantitative analysis of $[Ca^{2+}]_i$ elevation above basal levels elicited by BzATP (0.1 to 20 μM) in control (*black circle*) and in the presence of Saf (*white square*). The fit by Hill equation yielded an EC_{50} of 1.1 and 1.7 μM with BzATP alone and in co-application with Saf, respectively. Differences between BzATP and BzATP *plus* Saf were significant, $^{**}p < 0.01$. Data are obtained from at least 45 cells.

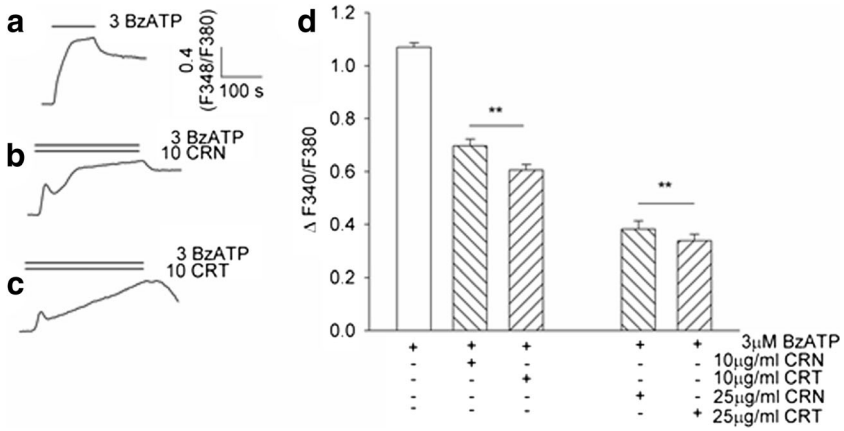

Fig. 7 Crocin and crocetin affects the BzATP-induced $[Ca^{2+}]_i$ elevation in HEK293-P2X7R cells. **a**–**c** Representative trace of $[Ca^{2+}]_i$ response induced by 3 μM BzATP alone (**a**), in the co-presence of 10 μg/ml crocin (*CRN*) (**b**), and 10 μg/ml crocetin (*CRT*) (**c**). **d** Quantitative analysis of $[Ca^{2+}]_i$ elevation above basal levels elicited by *BzATP* in control solution and in the presence of 10 and 25 μg/ml of CRN and CRT. $^{**}p < 0.01$ with respect to 3 μM BzATP alone for both CRN and CRT. Data were obtained from at least 45 cells

washout of BzATP and Saf (Fig. 8c). The summarized results demonstrate that Saf was able to reduce the inward current amplitude to about 30 %, analyzed during 3 μM BzATP application (Fig. 8d).

Discussion

In this study, we show that low amounts of saffron extract positively influence the cell viability of two different retinal cell cultures: mouse primary retinal cells and mouse retinal photoreceptor-derived 661W cells, both stressed by relatively high concentrations of ATP. Previous studies have demonstrated that extracellular ATP contributes to photoreceptor degeneration in rodents through excessive activation of P2 purinoreceptors. The involvement of P2X7Rs in retinal degeneration has been also documented in BALBCrds (retinal degeneration slow) mice [35]. In this work, we provide direct evidence of P2X7R expression in the mouse retinal photoreceptor-derived 661W cell line. Using the Western blotting technique, we identified the receptor with an apparent molecular weight of 68 kDa; a small extra band immediately beneath the denser band is consistent with the notion that the receptor can appear with different glycosylation patterns linked to its maturation process [37]. This fact is further demonstrated by the Western blot analysis of the P2X7 biotinylated fraction of 661W cells, where only one band, corresponding to the P2X7 glycosylated membrane fraction, is observable.

The presence of P2X7Rs in 661W cells was confirmed by calcium imaging experiments. ATP application in the absence of extracellular Ca^{2+} induced a transient $[Ca^{2+}]_i$ elevation in only about 18 % of the cells indicating that extracellular Ca^{2+} entry was the main mechanism responsible for the ATP-

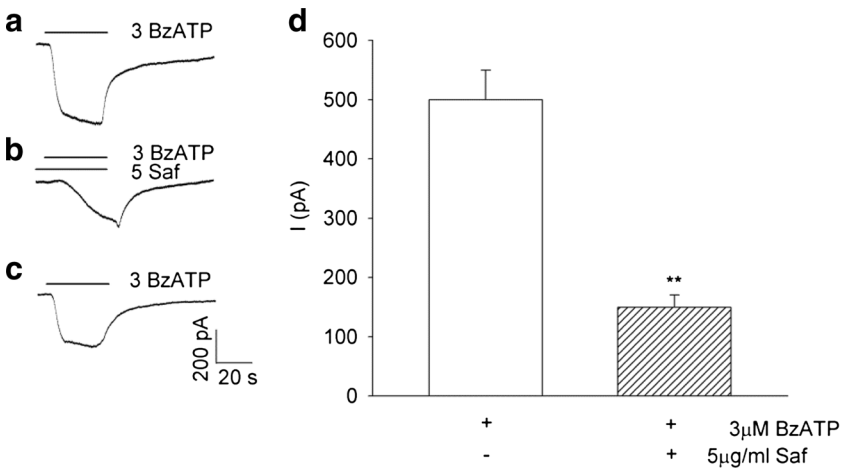

Fig. 8 Whole-cell current traces obtained from HEK293-P2X7R in the absence and in the presence of Saf. **a**–**c** BzATP-induced current traces obtained before, during application of 5 μg/ml Saf, and after Saf washout. Cells were clamped at a holding potential of −60 mV. **d** Histogram illustrating the significant block of 5 μg/ml Saf on BzATP-evoked currents. $^{**}p < 0.01$ with respect to 3 μM BzATP alone. Data are obtained from at least six single-cell experiments

induced $[Ca^{2+}]_i$ sustained signal. In addition, we observed that millimolar concentrations of ATP are necessary to induce $[Ca^{2+}]_i$ variations in mouse-retinal photoreceptor-derived cells, which is consistent with the low ATP affinity of P2X7R compared to other purinoreceptors (EC50 ≈ 1 mM ATP for mouse P2X7R [38]). Finally, we analyzed $[Ca^{2+}]_i$ variation in the presence of BBG, oATP, and the selective P2X7R antagonist A438079. BBG is known as a potent antagonist with a 30- to 50-fold greater sensitivity for rat versus human or mouse P2X7Rs. oATP is an irreversible P2X7Rs inhibitor (1–2-h incubation) that also acts on other purinoreceptors, P2X1Rs and P2X2Rs, as well as on nuclear factor NF-kB and cytokine release. Differently, A438079 is a reversible antagonist, selective for P2X7Rs over other P2 receptors [39]. Additionally, this last compound exhibited little or no activity on many other membrane receptors and ion channels. Our results showed that all these antagonists were able to block the $[Ca^{2+}]_i$ increase in 661W cells. Moreover, removing the reversible A438079 restored the ability of ATP to induce $[Ca^{2+}]_i$ increase. Interestingly, Saf significantly reduced $[Ca^{2+}]_i$ level in 661W cells indicating that its protective action involves P2X7Rs.

Similar results were observed in HEK293 cells stably transfected with recombinant rat P2X7Rs. Saf treatment increased the cell viability and decreased $[Ca^{2+}]_i$ level induced by stimulations with ATP or BzATP. Whereas in vivo the ATP^{4-} form of ATP is the physiological ligand, it is well recognized that in vitro BzATP is a stable and potent P2X7R activator, with a 100 times higher sensitivity in rat than in mouse [40]. The differences in the properties observed between the P2X7Rs of different species are important. Many pharmacological results have been obtained by heterologous expression of the rat P2X7Rs, restricting the knowledge of the effects of antagonists in other species. In this work, we observed a good agreement on Saf properties between 661W cells (of mouse origin) and HEK293-P2X7R (of rat origin): cell viability increased ≈10 % whereas $[Ca^{2+}]_i$ level decreased ≈40 % in the presence of Saf. Moreover, we noted that Saf mainly affected the slow component of the calcium rise. The significance of the biphasic behavior and the blocking effect of one component alone involves important considerations on various assumptions concerning the receptor structure and/or the high and low affinity binding sites [30, 41]. This topic is very interesting and deserves to be treated separately in future studies. We also verified that Saf modulated cationic currents in HEK293-P2X7R cells. Rat P2X2 receptors were used to examine the specificity of Saf to reduce P2X7-mediated Ca^{2+} entry. To our knowledge, this is the first report describing the possible neuroprotective effect of Saf through the regulation of P2X7R-mediated neuronal damage. The findings that the ATP-induced cell damage was almost abolished by the use of specific antagonists in both 661W cells and HEK293-P2X7R and the fact that Saf did not influence the recombinant P2X2-mediated response strongly suggest that P2X7R is a molecular target of Saf action. However, because of the partial effect of Saf on cell viability and P2X7R-mediated Ca^{2+} entry, we cannot consider the inhibiting effect of Saf on P2X7R as an exclusive mechanism of action.

The contribution of Saf in regulating the severity of neurodegeneration is under investigation. Saffron has been tested in an animal model of light-induced photoreceptor degeneration (light-induced damage (LD)) and in AMD patients. In both LD and AMD rats, oxidative stress plays a relevant role and a direct antioxidant activity of its main active components, crocins and crocetin, can be hypothesized. In this paper, we tested the efficiency of these components as antagonists of P2X7Rs. Calcium imaging experiments showed an effect of both crocins and crocetin in reducing Ca^{2+} entry on HEK293-P2X7R cells. However, results present in the literature suggest that the action of saffron can be more complex [22] and includes the modulation of gene expression [26, 27], e.g., the downregulation of genes involved in neuroinflammation (chemokines) and reduce microglia activation (paper in preparation). Recently, the identification of purinergic receptors on microglia has driven a strong debate on the pivotal role played by microglia and local ATP release as an injury signal in the process of aging and age-related diseases such as AMD [42, 43]. In this scenario, our data showing that Saf directly reduces the $[Ca^{2+}]_i$ response evoked by purinergic P2X7R stimulation unravels a novel mechanism through which Saf may exert its protective role in neurodegeneration. The next step will be to test saffron efficiency on the modulation of P2X7R in animal models like LD or AMD mice.

Another important issue that remains to be addressed in detail is the physiological significance of these results. In the brain, the P2X7R has been proposed to be involved in the signaling cascade leading to neuroinflammation and neurodegeneration [42, 44]. How the receptor contributes to these processes is not yet unequivocally verified. There is in vitro evidence that P2X7R contributes to regulate the inflammatory and degenerative responses by stimulating the synthesis and release of various cytokines and chemokines. Given the importance of $[Ca^{2+}]_i$ elevation in the biochemical cascades leading to apoptotic cell death [45], and because of the correlation of P2X7R-mediated cell death with the pore configuration of the receptor [46], it is tempting to speculate that the ability of Saf to inhibit the P2X7R-mediated $[Ca^{2+}]_i$ rise could interact with the structure of P2X7 pore involved in apoptotic cell death.

Acknowledgments We wish to thank Dr. Maria Maggi (HN s.r.L.) and Lab of Analytical Chemistry, University of L'Aquila, for performing the chemical analysis. We thank Dr. Joachim Scholz-Starke (IBF-CNR, Italy) for critical comments on the manuscript. The technical assistance of Francesca Quartino and Alessandro Barbin (IBF-CNR, Italy) was highly appreciated. This study was supported by MIUR-PRIN (2010–2011) research grant to SB.

Compliance with ethical standards The experiments were performed in compliance with the Animal Care and Use Committee guidelines and in accordance with the ARVO Statement for the Use of Animals in Ophthalmic and Vision Research.

Competing interest Prof. Bisti holds a non-remunerative relationship with "Hortus Novus s.r.l.," the company that provided the saffron used in this study. All the other authors declare that they have no competing interests.

References

1. Housley GD, Bringmann A, Reichenbach A (2009) Purinergic signalling in special senses. Trends Neurosci 32:128–141
2. Shen J, Yang X, Dong A, Petters RM, Peng YW, Wong F, Campochiaro P (2005) Oxidative damage is a potential cause of cone cell death in retinitis pigmentosa. J Cell Physiol 203:457–464
3. Puthussery T, Fletcher E (2009) Extracellular ATP induces retinal photoreceptor apoptosis through activation of purinoceptors in rodents. J Comp Neurol 513:430–440
4. Fletcher EL (2010) Mechanisms of photoreceptor death during retinal degeneration. Optom Vis Sci 87:269–275
5. Braendle U, Guenther E, Irrle C, Wheeler-Schilling TH (1998) Gene expression of the P2X receptors in the rat retina. Mol Brain Res 59:269–272
6. Wheeler-Schilling TH, Marquordt K, Kohler K, Jabs R, Guenther E (2000) Expression of purinergic receptors in bipolar cells of the rat retina. Mol Brain Res 76:415–418
7. Wheeler-Schilling TH, Marquordt K, Kohler K, Guenther E, Jabs R (2001) Identification of purinergic receptors in retinal ganglion cells. Mol Brain Res 92:177–180
8. Jarvis MF, Khakh BS (2009) ATP-gated P2X cation-channel. Neuropharmacology 56:208–215
9. Nobile M, Monaldi I, Alloisio S, Ferroni S (2003) ATP-induced, sustained calcium signalling in cultured rat cortical astrocytes: evidences for non-capacitative, $P2X_7$ like-mediated calcium entry. FEBS Lett 538:71–76
10. Sperlàgh B, Vizi E, Wirkner K, Illes P (2006) $P2X_7$ receptors in the nervous system. Prog Neurobiol 78:327–346
11. Innocenti B, Pfeiffer S, Zrenner E, Kohler K, Guenther E (2004) ATP-induced non-neuronal cell permeabilization in the rat inner retina. J Neurosci 24:8577–8583
12. Vessey KA, Jobling AI, Greferath U, Fletcher EL (2012) The role of P2X7 receptor in the retina: cell signalling and disfunction. Retin Degenerative Deseases 723:813–819
13. Skaper SD, Debetto P, Giusti P (2010) The $P2X_7$ purinergic receptor: from physiology to neurological disorders. FASEB J 24:337–345
14. Surprenant A, Rassendren F, Kawashima E, North RA, Buell G (1996) The cytolytic P2Z receptor for extracellular ATP identified as a P2X receptor (P2X7). Science 272:735–738
15. Zhang X, Zhang M, Laties AM, Mitchell CH (2005) Stimulation of P2X7 receptors elevates Ca^{2+} and kills retinal ganglion cells. Invest Ophthalmol Vis Sci 46:2183–2191
16. Notomi S, Hisatomi T, Murakami Y, Terasaki H, Sonoda S, Asato R, Takeda A, Ikeda Y, Enaida H, Sakamoto T, Ishibashi T (2013) Dynamic increase in extracellular ATP accelerates photoreceptor cell apoptosis via ligation of P2RX7 in subretinal hemorrhage. PLoS ONE 439:90–95
17. Giaccio M (2004) Crocetin from saffron: an active component of an ancient spice. Crit Rev Food Sci Nutr 44:155–172
18. Hosseinzadeh H, Sadeghnia HR, Ziaee T, Danaee A (2005) Protective effect of aqueous saffron extract (Crocus sativus L.) and crocin, its active constituent, on renal ischemia-reperfusion-induced oxidative damage in rats. J Pharm Sci 8:387–393
19. Pitsikas N, Boultadakis A, Georgiadou G, Tarantilis PA, Sakellaridis N (2008) Effects of the active constituents of Crocus sativus L., crocins, in an animal model of anxiety. Phytomedicine 15:1135–1139
20. Hosseinzadeh H, Younesi HM (2002) Antinociceptive and anti-inflammatory effects of Crocus sativus L. stigma and petal extracts in mice. BMC Pharmacol 2002 2:7
21. Escribano J, Alonso GL, Coca-Prados M, Fernandez JA (1996) Crocin, safranal and picrocrocin from saffron (Crocus sativus L.) inhibit the growth of human cancer cells in vitro. Cancer Lett 100: 23–30
22. Maccarone R, Di Marco S, Bisti S (2008) Saffron supplement maintains morphology and function after exposure to damaging light in mammalian retina. Invest Ophthalmol Vis Sci 49:1254–1261
23. Falsini B, Piccardi M, Minnella A, Savastano C, Capoluongo E, Fadda A, Balestrazzi E, Maccarone R, Bisti S (2010) Influence of saffron supplementation on retinal flicker sensitivity in early age-related macular degeneration. Invest Ophthalmol Vis Sci 51:6118–6124
24. Piccardi M, Marangoni D, Minnella AM, Savastano MC, Valentini P, Ambrosio L, Capoluongo E, Maccarone R, Bisti S, Falsini B (2012) A longitudinal follow-up study of saffron supplementation in early age-related macular degeneration: sustained benefits to central retinal function. Evid Based Complement Alternat Med ID 429124
25. Marangoni D, Falsini B, Piccardi M, Ambrosio L, Minnella AM, Savastano MC, Bisti S, Maccarone R, Fadda A, Mello E, Concolino P, Capoluongo E (2013) Functional effect of saffron supplementation and risk genotypes in early age-related macular degeneration: a preliminary report. J Transl Med 11:228
26. Natoli R, Zhu Y, Valter K, Bisti S, Eells J, Stone J (2010) Gene and noncoding RNA regulation underlying photoreceptor protection: microarray study of dietary antioxidant saffron and photobiomodulation in rat retina. Mol Vis 16:1801–1822
27. Bisti S, Maccarone R, Falsini B (2014) Saffron and retina: neuroprotection and pharmaco-kinetics. Vis Neurosci 31:355–361
28. Fox DA, Poblenz AT, He L (1999) Calcium overload triggers rod photoreceptor apoptotic cell death in chemical-induced and inherited retinal degenerations. Ann N Y Acad Sci 893:282–285
29. Tan E, Ding XQ, Saadi A, Agarwal N, Naash MI, Al-Ubaidi MR (2004) Expression of cone-photoreceptor-specific antigens in a cell line derived from retinal tumors in transgenic mice. Invest Ophthalmol Vis Sci 45:764–768
30. Alloisio S, Di Garbo A, Barbieri R, Bozzo L, Ferroni S, Nobile M (2010) Evidences for two conductive pathways in P2X7 receptor: differences in modulation and selectivity. J Neurochem 113:796–806
31. Lowry OH, Rosebrough NJ, Farr AL, Randall NJ (1951) Protein measurement with the Folin phenol reagent. J Biol Chem 193(1): 265–275
32. Grynkiewicz G, Poenie M, Tsien RY (1985) A new generation of Ca^{2+} indicators with greatly improved fluorescence properties. J Biol Chem 260:3440–3450
33. Mackey AM, Sanvicens N, Groeger G, Doonan F, Wallace D, Cotter TG (2008) Redox survival signaling in retina-derived 661W cells. Cell Death Differ 15:1291–1303
34. Yang D, Elner SG, Clark AJ, Hughes BA, Petty HR, Elner VM (2011) Activation of P2X receptors induces apoptosis in human retinal pigment epithelium. Invest Ophthalmol Vis Sci 52:1522–1530
35. Franke H, Klimke K, Brinckmann U, Grosche J, Francke M, Sperlagh B, Reichenbach A, Liebert UG, Illes P (2005) P2X(7)

receptor-mRNA and -protein in the mouse retina; changes during retinal degeneration in BALBCrds mice. Neurochem Int 47:235–242
36. Jiang LH, Mackenzie AB, North RA, Surprenant A (2000) Brilliant Blue G selectively blocks ATP-gated rat P2X7 receptors. Mol Pharmacol 58:82–88
37. Di Virgilio F (2003) Novel data point to a broader mechanism of action of oxidized ATP: the P2X7 receptor is not the only target. Br J Pharmacol 140(3):441–443
38. Nelson DW, Gregg RJ, Kort ME, Perez-Medrano A, Voight EA, Wang Y, Grayson G, Namovic MT, Donnelly-Roberts DL, Niforatos W, Honore P, Jarvis MF, Faltynek CR, Carroll WA (2006) Structure-activity relationship studies on a series of novel, substituted 1-benzyl-5-phenyltetrazole P2X7 antagonists. J Med Chem 49:3659–3666
39. Young TM, Pelegrin P, Surprenant A (2007) Amino acid residues in the P2X7 receptor that mediate differential sensitivity to ATP and BzATP. Mol Pharm 71:92–100
40. North RA, Surprenant A (2000) Pharmacology of cloned P2X receptors. Annu Rev Pharmacol Toxicol 40:563–580
41. Yan Z, Khadra A, Li S, Tomic M, Sherman A, Stojilkovic SS (2010) Experimental characterization and mathematical modeling of P2X7 receptor channel gating. J Neurosci 30:14213–14224
42. Wong WT (2013) Microglia aging in the healthy CNS: phenotypes, drivers and rejuvenation. Front Cell Neurosci 7(22):1–13
43. Karlstetter M, Scholz R, Rutar M, Wong WT, Provis JM (2015) Retinal microglia: just bystander or target for therapy? Prog Retin Eye Res 45:30–57
44. Wang X, Arcuino G, Takano T, Lin J, Peng WG, Wan P, Li P, Xu Q, Liu QS, Goldman SA, Nedergaard M (2004) P2X7 receptor inhibition improves recovery after spinal cord injury. Nat Med 10:821–827
45. Franklin JL, Johnson EM Jr (1992) Suppression of programmed neuronal death by sustained elevation of cytoplasmic calcium. Trends Neurosci 15:501–508
46. Virginio C, MacKenzie A, North RA, Surprenant A (1999) Kinetics of cell lysis, dye uptake and permeability changes in cells expressing the rat P2X7 receptor. J Physiol 519:335–346